Supporting Information

Terashima et al. 10.1073/pnas.1207118109

SI Materials and Methods

Generation of Artificial microRNA and RNAi Mutants. Plasmid construction and generation of RNAi and artificial microRNA (amiRNA) lines was done as as described in ref. 1. The oligonucleotides used for amiRNA-anr1 were 5′-tagtCGGGTCTACATTGGCTACGTAtctcgctgatcggcaccatgggggtggtggtgatcagcgcta TACGAAGCCAATGTAGACCCGg-3′ and 5′-ctagcCGGGTCTACATTGGCTTCGTAtagcgctgatcaccaccacccccatggtgccgatcagcgaga TACGTAGCCAATGTAGACCCGa-3′ (uppercase letters indicate mi-RNA*/mi-RNA sequences). The generated RNAi-*cas* plasmid was transformed into the 21gr strain using biolistic transformation, whereas the amiRNA-*anr1* was transformed into the cell wall-deficient *cw15-arg7* strain using glass beads, as previously described (2).

RT-PCR. RT-PCR analysis of ami-RNA *tef7* was performed as described in ref. 3, with the following primers:

ANR1 F: AAGCAGGTGAAGGTGTCGT
ANR1 R: GGAGTCCTTCTCCTTAATGACC
TUB1 F: TGCCTGCAGGGCTTCCAGG
TUB1 R: GGGATCCACTCGACGAAGTA.

Mass Spectrometry. Mass spectrometric analyses were performed as previously described (3), except that the ^{15}N labeling approach was used. OMSSA (4) and qTrace (3) programs were used for protein identification and quantitation, respectively, using Proteomatic (5). OMSSA parameters were used as previously described (3) (with 1% false-positive rate and 5 ppm mass accuracy filters), with the additional second run with the precursor and product ion search types set to "N15." Additionally, "protein groups" were applied to the OMSSA results to group identified nonunique peptides that are shared by multiple proteins. The comma-separated values (CSV) files containing the identified peptides from the two OMSSA runs were used together for target masses for qTrace. Settings were used as described by Terashima et al. (3), with the following filtering steps: (*i*) require MS2 identifications, (*ii*) add protein names/group information, (*iii*) pick most abundant bands, and (*iv*) require both sister peptides. After the protein ratios were determined, results were filtered to keep only the quantified proteins with at least two peptide/band/charge (PBC) combinations and a relative SD of 0.6 or smaller. Protein information was also extracted after filtering with "pick most abundant bands" to find those proteins where the peptide mass was present in only one isotopic form. Those proteins where the peptide was present in one isotope form consistently for at least two tryptic peptides were kept. Finally, the list was filtered to include only proteins from the 996 chloroplast-localized proteins (6) to exclude mitochondrial or cytoplastic proteins. For the sucrose density gradients (SDGs), the same filters were used except that both sister peptides were not required, a relative SD of 0.8 was required, and the quantified proteins were filtered for 10 or more spectral counts instead of filtering for PBC counts.

1. Petroutsos D, et al. (2011) The chloroplast calcium sensor CAS is required for photoacclimation in *Chlamydomonas reinhardtii*. *Plant Cell* 23:2950–2963.
2. Kindle KL, Schnell RA, Fernández E, Lefebvre PA (1989) Stable nuclear transformation of *Chlamydomonas* using the *Chlamydomonas* gene for nitrate reductase. *J Cell Biol* 109:2589–2601.
3. Terashima M, Specht M, Naumann B, Hippler M (2010) Characterizing the anaerobic response of *Chlamydomonas reinhardtii* by quantitative proteomics. *Mol Cell Proteomics* 9:1514–1532.
4. Geer LY, et al. (2004) Open mass spectrometry search algorithm. *J Proteome Res* 3: 958–964.
5. Specht M, Kuhlgert S, Fufezan C, Hippler M (2011) Proteomics to go: Proteomatic enables the user-friendly creation of versatile MS/MS data evaluation workflows. *Bioinformatics* 27:1183–1184.
6. Terashima M, Specht M, Hippler M (2011) The chloroplast proteome: A survey from the *Chlamydomonas reinhardtii* perspective with a focus on distinctive features. *Curr Genet* 57:151–168.

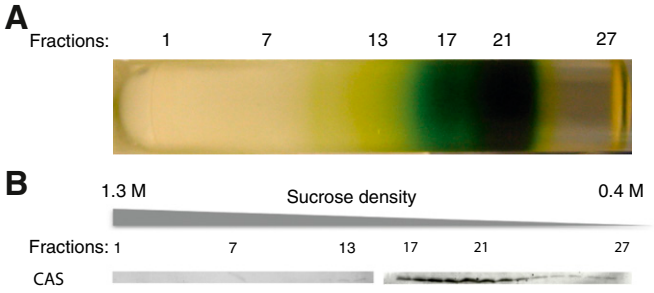

Fig. S1. (*A*) SDG separation of ΔPSI anaerobic thylakoids into 27 (F1–F27) fractions. (*B*) Immunoblot detection of CAS among the 27 TCA-precipitated fractions confirms its shift to the lower-density region (peaking around F19) of the SDG in ΔPSI.

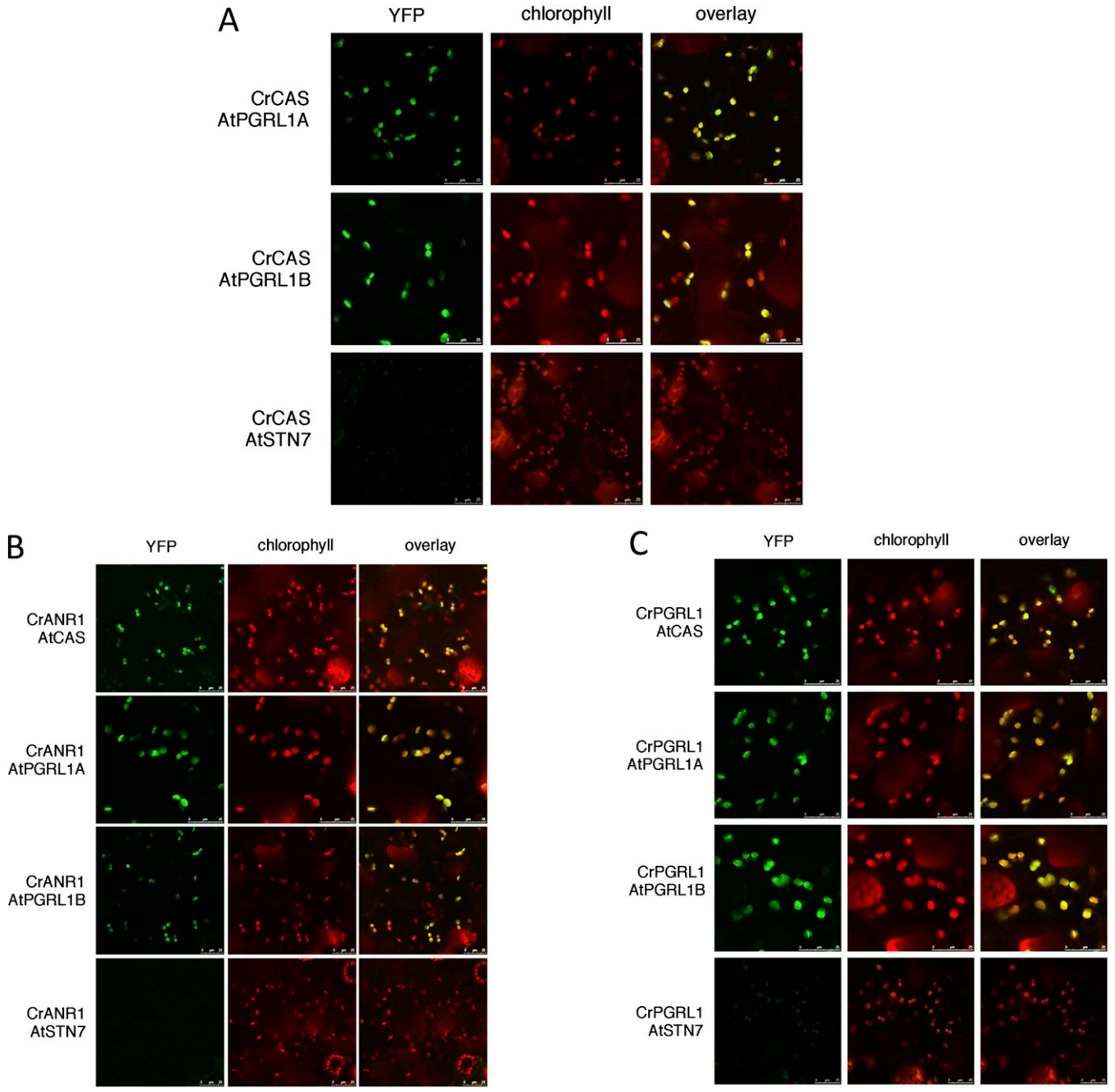

Fig. S2. (*A*) Bimolecular fluorescence complementation (BiFC) interaction analyses of *Chlamydomonas reinhardtii* CAS with AtPGRL1A/B and AtSTN7 expressed in *Nicotiana benthamiana* leaves. In independent experiments it was proven that an AtSTN7-GFP fusion was targeted into chloroplasts after transfection of *N. benthamiana* leaves. (*B*) BiFC interaction analyses of *C. reinhardtii* ANR1 with AtCAS, AtPGRL1A/B, and AtSTN7 expressed in *N. benthamiana* leaves. (*C*) BiFC interaction analyses of *C. reinhardtii* PGRL1 with AtCAS, AtPGR5, AtPGRL1A/B, and AtSTN7 expressed in *N. benthamiana* leaves.

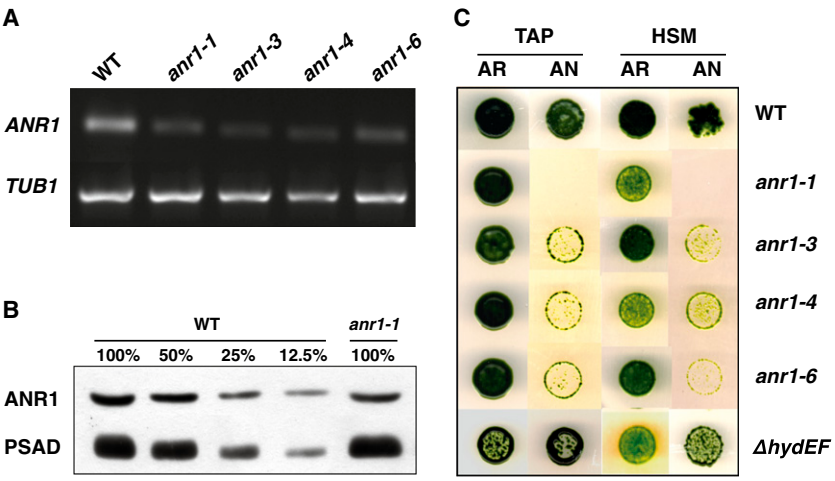

Fig. S3. Transcript and protein analyses by RT-PCR and immunoblotting reveal reduced levels of *ANR1* in the *ami-RNA-anr1* lines compared with the WT, and spot tests disclose attenuated growth under anaerobic conditions for the mutant lines. (*A*) *ANR1* transcript levels are decreased in all four *ami-RNA-anr1* knockdown lines 1, 3, 4, and 6. Transcript levels for tubulin (*TUB1*) were used as a loading control. (*B*) Immunoblot analyses of anaerobic whole-cell extracts from WT and *ami-RNA-anr1-1* reveal that ANR1 levels are approximately 50% of levels seen in WT. Five micrograms of chlorophyll equals 100%. Photosystem I subunit D (PSAD) was used as a loading control, and levels are not compromised in the *ami-RNA-anr1* mutant. (*C*) A total of 1×10^4 cells were spotted on either Tris-acetate-phosphate (TAP) media or high-salt media (HSM) plates and grown under aerobic (AR) or anaerobic (AN) conditions under 50 μE m^{-2} s^{-1} light. The WT and ΔHYDEF strain lacking in hydrogenase (1) exhibit no dramatic differences between AR and AN conditions on each growth media, whereas the *ami-RNA-anr1* knockdown lines have severe growth defect only under AN conditions. The differences in phenotype between the *anr1* knockdown lines and the ΔHYDEF strain suggests that ANR1 is not directly related to hydrogen production, but some other aspect of the anaerobic response mechanism.

1. Dubini A, Mus F, Seibert M, Grossman AR, Posewitz MC (2009) Flexibility in anaerobic metabolism as revealed in a mutant of *Chlamydomonas reinhardtii* lacking hydrogenase activity. *J Biol Chem* 284:7201–7213.

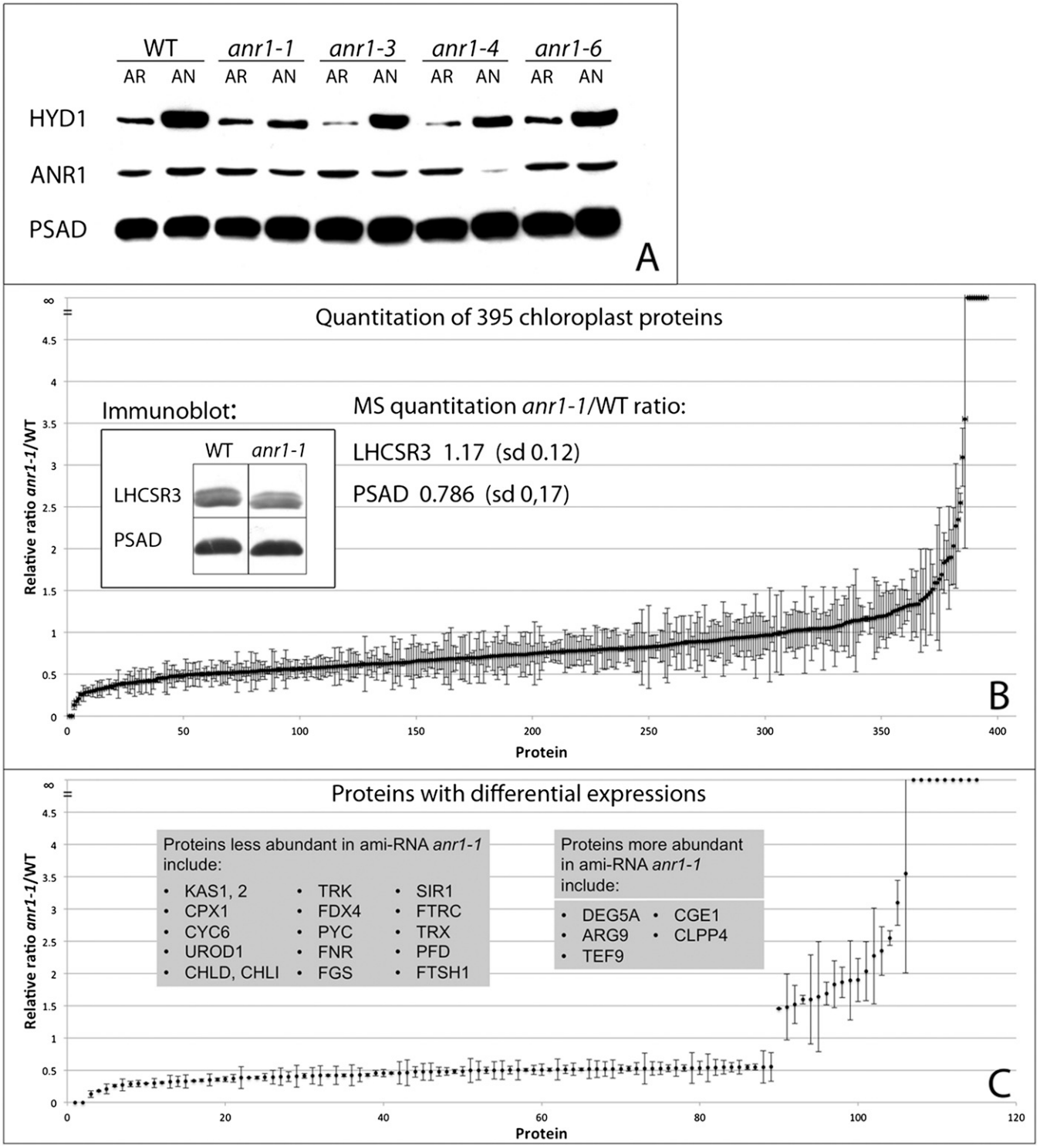

Fig. S4. Immunoblot analyses of *ami-RNA-anr1* lines and relative abundance of 395 anaerobic *ami-RNA-anr1-1* to anaerobic WT chloroplast proteins quantified using mass spectrometry. (*A*) Immunoblot analyses of aerobic (AR) and anaerobic (AN; 4 h argon bubbling) whole cells from WT and *ami-RNA-anr1* knockdown lines (*anr1-1*, *anr1-3*, *anr1-4*, and *anr1-6*) display lower levels of the hydrogenase (HYD1) protein. The anaerobic induction of the ANR1 protein is also not observed in the knockdown lines. PSAD levels are not compromised in the *ami-RNA-anr1* mutant. Five-microgram chlorophyll whole cells were loaded. (*B*) For quantitative analyses using mass spectrometry, the mutant line and WT (^{15}N-labeled) were bubbled for 8 h with argon to induce anaerobic conditions, and the chloroplasts were isolated. Five μg of chlorophyll from each sample were mixed and separated on an SDS/PAGE, followed by Coomassie staining. Bands and the spaces between the visible bands were cut out, digested with trypsin, and the peptides measured by the LTQ Orbitrap XL hybrid Fourier Transform Mass Spectrometer (Thermo Scientific) followed by identification using OMSSA and quantitation with qTrace (1). Quantitation results were coupled to MS^2 identifications, and the results were filtered to include those with two or more peptide/band/charge (PBC) combinations. Proteins only present in one isotopic form for quantitation (resulting in a ratio of zero or infinity) required at least two proteotypic peptides to ensure that the observation is not due to a mass shift from a modification occurring under one condition. The depicted results represent data from four separate MS runs, obtained from three separate biological

Legend continued on following page

samples for each strain. Each dot represents a quantified protein. *Inset*: Immunoblot detection demonstrates comparable abundance to the MS-quantified ratios. LHCSR3, stress-related chlorophyll a/b binding protein 3; PSAD, PS1 protein subunit PsaD. (*C*) Selected proteins with varying ratios between *ami-RNAi-anr1-1* and WT. Some proteins that are less or more abundant in the mutant line are highlighted in the gray box. CHLD and CHLI, magnesium chelatase subunits D and I; CPX1, coproporphyrinogen III oxidase; CYC6, cytochome c6; FDX4, ferredoxin 4; FNR, ferredoxin-NADP$^+$ reductase; KAS, β-keto-acyl-acyl carrier protein; PYC, pyruvate carboxylase; SIR1, ferredoxin-sulfite reductase 1; TRK, transketolase; UROD1, uroporphyrinogen-III decarboxylase.

1. Terashima M, Specht M, Naumann B, Hippler M (2010) Characterizing the anaerobic response of Chlamydomonas reinhardtii by quantitative proteomics. *Mol Cell Proteomics* 9: 1514–1532.

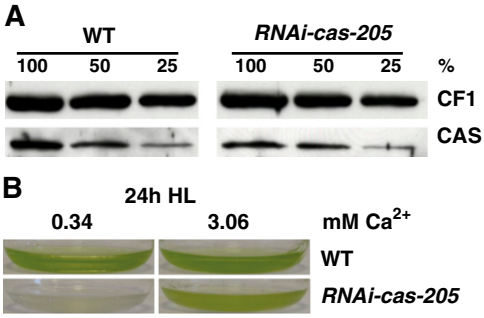

Fig. S5. (*A*) Quantification of CAS protein amounts in thylakoids isolated from WT (21gr) and *RNAi-cas-205*, grown in TAP at 20 μE m^{-2} s^{-1}, upon SDS/PAGE fractionation and immunoblot analysis (100% equals 7.5 μg of chlorophyll per lane; CF1 signal served as loading control). (*B*) WT and *RNAi-cas-205* grown in TAP medium at 20 μE m^{-2} s^{-1} were shifted to HSM and 200 μE m^{-2} s^{-1} for 24 h. The *RNAi-cas-205* culture containing normal Ca^{2+} levels (0.34 mM) was very photosensitive, and this sensitivity was rescued by increased Ca^{2+} in the medium (3.06 mM), as has been described with other *cas* mutants (1). The WT culture grew equally well at 0.34 and 3.06 mM Ca^{2+}.

1. Petroutsos D, et al. (2011) The chloroplast calcium sensor CAS is required for photoacclimation in *Chlamydomonas reinhardtii*. *Plant Cell* 23:2950–2963.

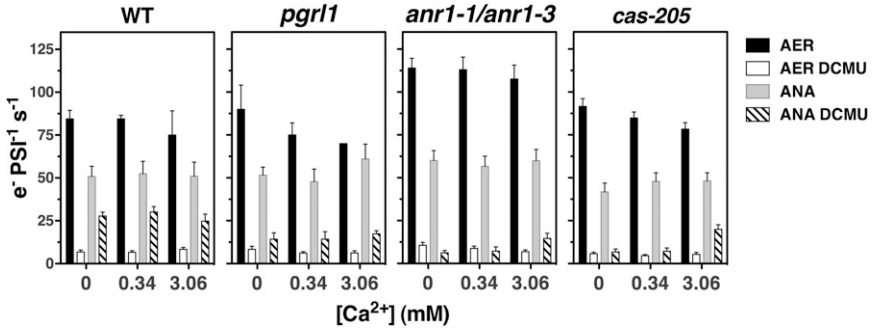

Fig. S6. Down-regulation of ANR or CAS results in diminished cyclic electron flow (CEF), which is partially restored by increasing the extracellular Ca^{2+} concentration. Linear electron flow (LEF) and CEF activity under aerobic and anaerobic conditions in WT (21gr and *cw15-arg7*), *pgrl1*, *amiRNA-anr1-1*, *amiRNA-anr1-3*, and *RNAi-cas-205* grown in photoheterotrophic medium containing the indicated Ca^{2+} concentration. Data are expressed as electrons per photosystem I per second. Data (±SD) refer to five measurements from three biological replicates for WT and *pgrl1* (10 and 13 measurements from 5 and 7 biological replicates for *cas-205* and *anr1-3/anr1-5*, respectively).

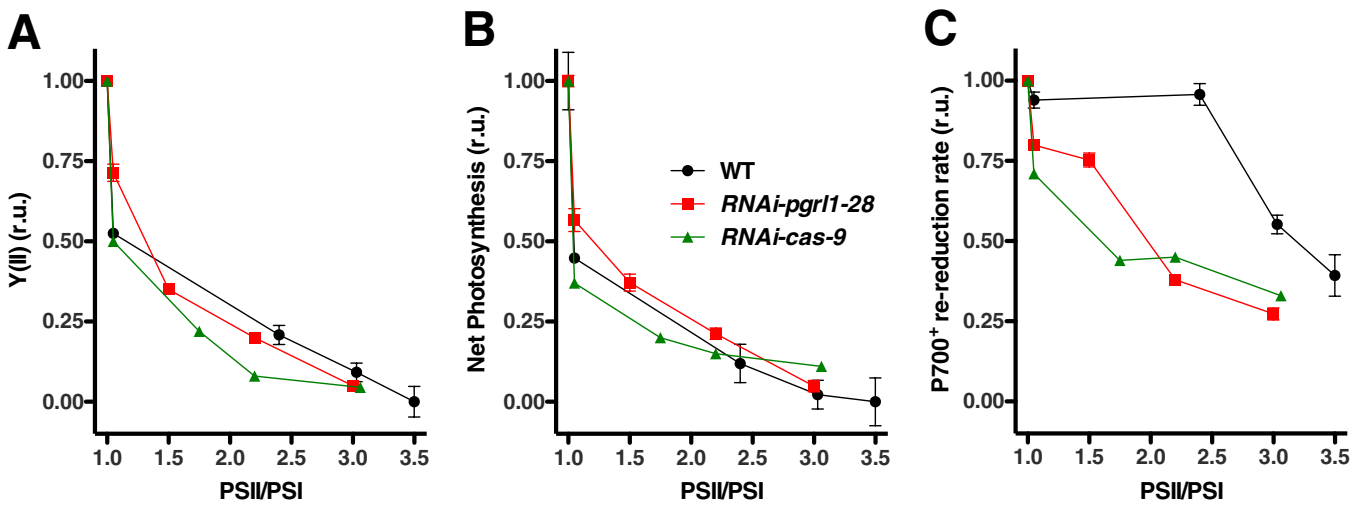

Fig. S7. CAS is required for CEF under iron-limited conditions. WT (CC-124) and *RNAi-cas-9* grown in iron-replete TAP medium were shifted to iron-depleted TAP and quantum yield of PSII (Y(II); *A*), net photosynthesis (*B*), and $P700^+$ rereduction rate (*C*) were measured over a 4-d period and plotted against PSII/PSI ratio; PSI and PSII content was estimated spectroscopically from changes in the amplitude of the fast phase (100 μs) of the ECS (electrochromic shift) signal at 520–546 nm upon excitation with a saturating laser flash. PSII content was evaluated form the decrease in the ECS amplitude upon addition of 3-(3,4-dichlorophenyl)-1,1-dimethylurea (DCMU) (10 μM) and hydroxylamine (1 mM) to prevent PSII charge separation. PSI was estimated as the fraction of ECS signal that remained upon cell poisoning with these inhibitors. PSI complex is a specific target of iron starvation, whereas PSII remains unaltered, accordingly the PSII/PSI ratio increases during these experimental conditions, as previously described (1). The *RNAi-cas-9* has *ca*. 50% reduced protein CAS levels compared with WT (2). For comparison reasons the graphs also include the data for the *pgrl1* knockdown line *RNAi-pgrl1-28*, described previously (1). Data represent means (±SD) of three independent experiments for WT and *RNAi-pgrl1-28*.

1. Petroutsos D, et al. (2009) PGRL1 participates in iron-induced remodeling of the photosynthetic apparatus and in energy metabolism in *Chlamydomonas reinhardtii*. *J Biol Chem* 284: 32770–32781.
2. Petroutsos D, et al. (2011) The chloroplast calcium sensor CAS is required for photoacclimation in *Chlamydomonas reinhardtii*. *Plant Cell* 23:2950–2963.

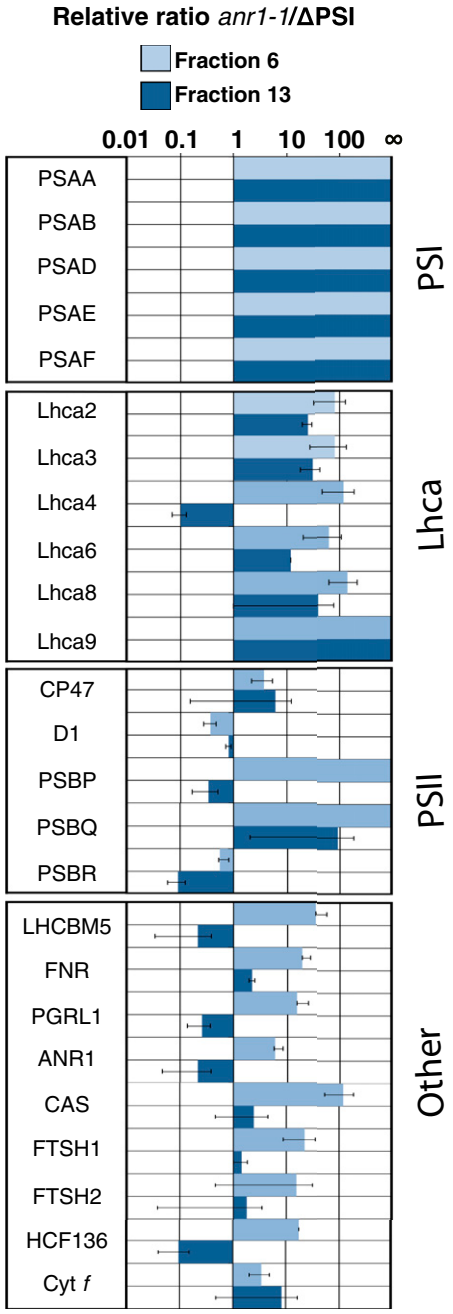

Fig. S8. Relative quantitation of proteins identified from fraction 6 and 13 of the SDG. WT (*cw15-arg7*) or ami-RNAi *anr1-1* fraction 6 or 13 was compared with the same fraction from the ^{15}N-labeled ΔPS1 strain. Equal volumes (30 μL) from each sample were mixed and separated on a small SDS/PAGE, followed by Coomassie staining. Bands and the spaces between the visible bands were cut out, digested with trypsin, and the peptides measured by the LTQ Orbitrap XL hybrid FTMS, followed by identification using OMSSA and quantitation with qTrace (1). Quantitation results were coupled to MS^2 identifications, and the results were filtered to include those with two or more PBC combinations. Relative quantitation results for proteins quantified under all comparisons: WT vs. ΔPS1 and ami-RNAi *anr1-1* vs. ΔPS1, fractions 6 and 13 for each strain combination. The results for ami-RNAi *anr1-1* vs. ΔPS1 comparison stem from three biological replicate; the results for WT vs. ΔPS1 comparison stem from two biological replicate. ANR1, anaerobic response protein 1; CAS, rhodanese-like calcium-sensing receptor; Cytb6, cytochrome b_6; Cytb6/f subunit IV, cytochrome b_6f complex subunit IV; Cytf, cytochrome f; FNR, ferredoxin-NADP$^+$ reductase; FTSH1-2, FtsH membrane metalloproteases; Lhca1-9, light-harvesting proteins of PS1; Lhcb4-5, light-harvesting proteins of PS2; LHCBM1-9, major light-harvesting proteins of PS2; PSAA-PSAL, PS1 reaction center subunits; PETC, the cytochrome b_6f complex Rieske iron sulfur cluster protein; PETO, cytochrome b_6f complex subunit V; PGRL1, PGR5-like protein 1.

1. Terashima M, Specht M, Naumann B, Hippler M (2010) Characterizing the anaerobic response of Chlamydomonas reinhardtii by quantitative proteomics. *Mol Cell Proteomics* 9: 1514–1532.

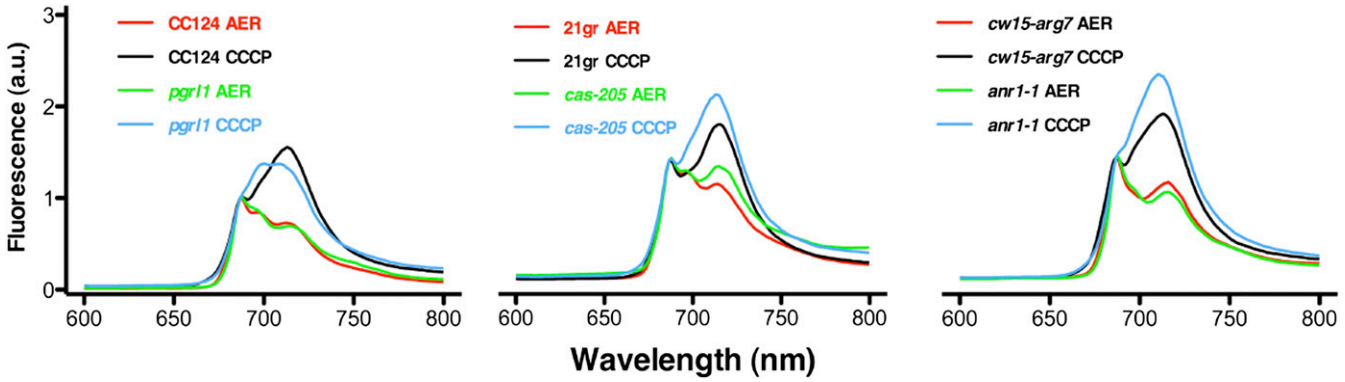

Fig. S9. None of *pgrl1*, *anr1*, and *cas* is impaired in state transitions. The ability of *pgrl1*, *anr1*, and *cas* to perform state transitions was checked using low temperature (77 K) fluorescence, as described previously (1). State I conditions were established by vigorous shaking of the cells in the dark for 4 h; for establishment of state II, cells were incubated in the dark for 20 min in the presence of 10 μM carbonyl cyanide 3-chlorophenylhydrazone.

1. Petroutsos D, et al. (2009) PGRL1 participates in iron-induced remodeling of the photosynthetic apparatus and in energy metabolism in *Chlamydomonas reinhardtii*. *J Biol Chem* 284: 32770–32781.

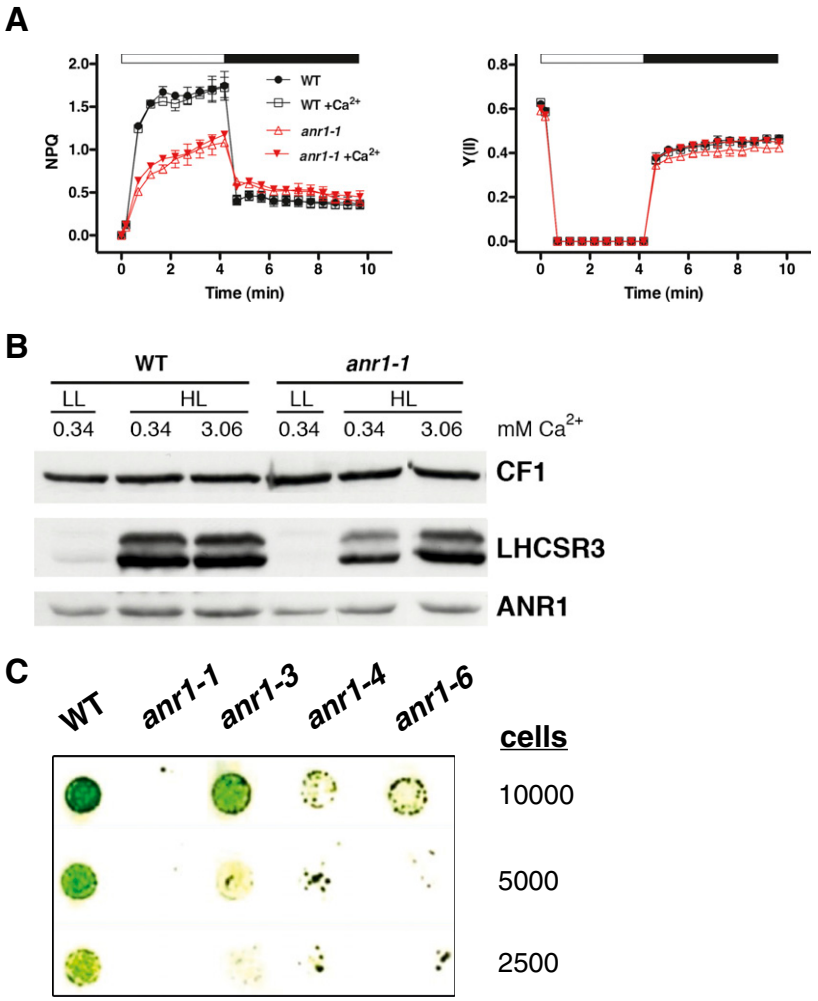

Fig. S10. Nonphotochemical quenching (NPQ) induction and LHCSR3 light-dependent expression are impaired in *amiRNA-anr1-1*. (*A*) WT (*cw15-arg7*) and *amiRNA-anr1-1* grown in TAP LL (20 μE m^{-2} s^{-1}) were set at 2.5 μg chlorophyll/mL and shifted for 4 h to HL (200 μE m^{-2} s^{-1}) and HSM containing 0.34 or 3.06 mM $CaCl_2$. After the high light (HL) exposure the cells were dark-adapted for 20 min, and NPQ and the quantum yield of PSII were recorded during 4.2 min of illumination at 800 μE m^{-2} s^{-1} (open bar) followed by 5.5 min of darkness (filled bar), during which recovery of PSII and relaxation of NPQ was followed. Values plotted represent the means of three measurements ± SD. (*B*) Immunodection of LHCSR3 and ANR1 in whole-cell extracts of the experiment described above, after SDS/PAGE fractionation (2.5 μg of chlorophyll per lane; CF1 signal served as loading control). (*C*) Spot test comparing WT (*cw15-arg7*) and ami-RNA *anr1* knockdown lines on HSM plates incubated under 250 μE m^{-2} s^{-1} light show high-light sensitivity of the anr1 mutant lines. The cell numbers indicated in the figure refer to the total cell number spotted on the plate.

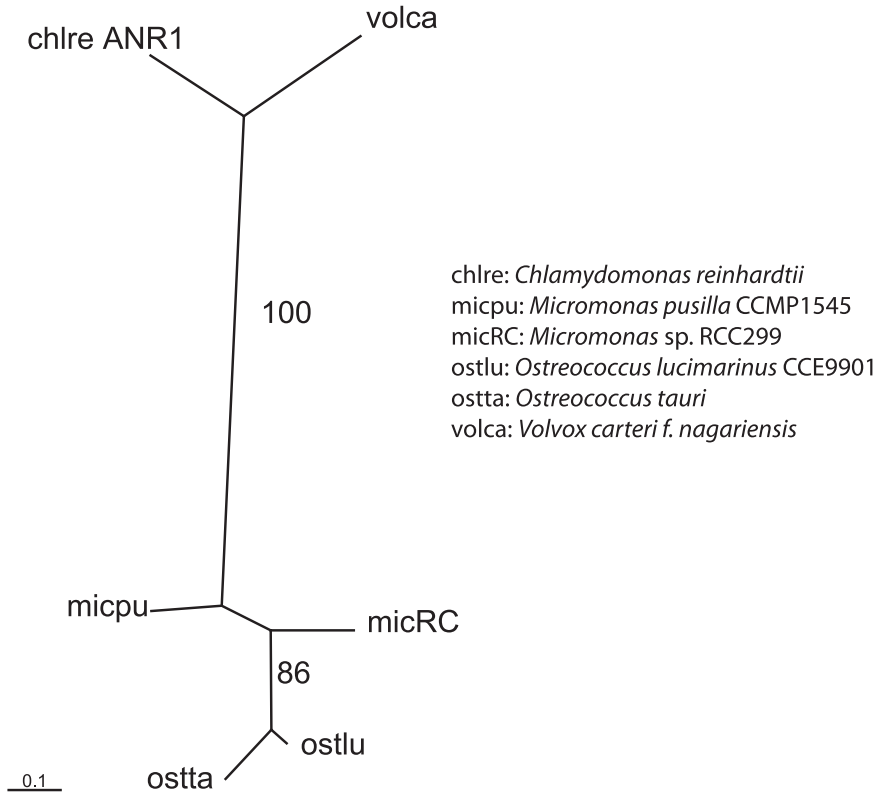

Fig. S11. Phylogenetic analysis shows ANR1 protein to be an algae-specific protein. Hits from National Center for Biotechnology Information blastp (all nonredundant GenBank coding DNA sequence (CDS) translations, protein databank (PDB), SwissProt, protein information resource (PIR), and poisson random field (PRF) excluding environmental samples from whole genome shotgun (WGS) projects) were aligned using clustralW, and amino acid positions that were unambiguously aligned were extracted (92 amino acids) from a total of five proteins (all annotated as hypothetical proteins). Proteins used for analysis were CHLNCDRAFT_52757, MICPUCDRAFT_45626, MICPUN_96511, Ot04g03510, OSTLU_15098, and VOLCADRAFT_120979. Maximum-likelihood tree was generated using the WAG+G model, as selected by ProtTest, with 100 bootstrap replicates.

Table S1. Statistical comparison of all column pairs of Fig. 3, performed by one-way ANOVA followed by the Tukey's multiple comparison test ($P < 0.01$)

		WT			*pgrl1*			*anr1-1/anr1-3*			*cas-205*		
Strain	mM Ca^{2+}	0	0.34	3.06	0	0.34	3.06	0	0.34	3.06	0	0.34	3.06
WT	0		No	No	Yes	Yes	Yes	Yes	Yes	Yes	Yes	Yes	Yes
	0.34	No		No	Yes	Yes	Yes	Yes	Yes	Yes	Yes	Yes	Yes
	3.06	No	No		Yes	Yes	Yes	Yes	Yes	Yes	Yes	Yes	No
pgrl1	0	Yes	Yes	Yes		No	No	Yes	Yes	No	Yes	Yes	Yes
	0.34	Yes	Yes	Yes	No		No	Yes	Yes	No	Yes	Yes	Yes
	3.06	Yes	Yes	Yes	No	No		Yes	Yes	No	Yes	Yes	Yes
anr1-1/ anr1-3	0	Yes	Yes	Yes	Yes	Yes	Yes		No	Yes	No	No	Yes
	0.34	Yes	Yes	Yes	Yes	Yes	Yes	No		Yes	No	No	Yes
	3.06	Yes	Yes	Yes	No	No	No	Yes	Yes		No	Yes	Yes
cas-205	0	Yes	Yes	Yes	Yes	Yes	Yes	No	No	No		No	Yes
	0.34	Yes	Yes	Yes	Yes	Yes	Yes	No	No	Yes	No		Yes
	3.06	Yes	Yes	No	Yes	Yes	Yes	Yes	Yes	Yes	Yes	Yes	

"Yes" denotes statistically significant difference.